Solar energy enhancement using down-converting particles: A rigorous approach

Ze'ev R. Abrams,[1,2] Avi Niv,[2] and Xiang Zhang[2,3,a)]
[1]*Applied Science and Technology, University of California, Berkeley, California 94720, USA*
[2]*NSF Nanoscale Science and Engineering Center, 3112 Etcheverry Hall, University of California, Berkeley, California 94720, USA*
[3]*Materials Science Division, Lawrence Berkeley National Laboratory, 1 Cyclotron Road, Berkeley, California 94720, USA*

(Received 26 January 2011; accepted 15 April 2011; published online 6 June 2011)

The efficiency of a single band-gap solar cell is specified by the Shockley-Queisser limit, which defines the maximal output power as a function of the solar cell's band-gap. One way to overcome this limit is by using a down-conversion process whereupon a high energy photon is split into two lower energy photons, thereby increasing the current of the cell. Here, we provide a full analysis of the possible efficiency increase when placing a down-converting material on top of a pre-existing solar cell. We show that a total 7% efficiency improvement is possible for a perfectly efficient down-converting material. Our analysis covers both lossless and lossy theoretical limits, as well as a thermodynamic evaluation. Finally, we describe the advantages of nanoparticles as a possible choice for a down-converting material. © *2011 American Institute of Physics*. [doi:10.1063/1.3592297]

I. INTRODUCTION

The efficiency of a single band-gap solar cell is constrained by matching the system's band-gap to the radiation spectrum of the sun. The Shockley-Queisser limit[1] of 31% for a single junction, semiconducting solar cell is possible for a material with a band-gap of 1.1–1.3 eV, in the range of many common semiconductors such as Silicon and Gallium-Arsenide. However, with a single-junction solar cell not all of the solar energy is utilized: some of the energy is lost to lower energy photons that are transparent to the semiconductor, and an additional portion is lost to the thermalization of higher energy photons. These losses can add up to more than 50% of the utilizable solar energy for a Silicon solar cell.[2] Various concepts have been proposed over the last 50 years to surpass this fundamental efficiency limit for a single-junction solar cell.[3,4] These concepts have included multi-junction solar cells, interband transitions, and up- and down-conversion.[4]

Down-conversion (DC) is intended to better utilize the free energy of photons with energy *higher* than the band-gap of the solar cell, which is otherwise lost to thermalization. In the DC process, first analyzed by Trupke *et al.*,[5] a separate material from the solar cell is used to split photons with energy at twice the band-gap energy into two lower energy photons, which are better matched to the solar cell's band-gap. DC is intended to increase the current of the solar cell by increasing the number of absorbed photons impinging upon the solar cell while retaining its voltage characteristics. This increase in current subsequently increases the overall efficiency of the system. The DC process can be considered as modifying the solar spectrum to better match the solar cell properties, as opposed to changing the solar cell itself, enabling the efficiency increase of the underlying solar cell beyond the Shockley-Quiesser limit.

The analysis of a simplified DC system was first proposed by Trupke *et al.*[5] and further improved upon by Badescu *et al.*[6,7] Their analyses were based on a model system that includes a hypothetical solar cell that only absorbs photons between its band-gap (E_g) and double its band-gap ($2E_g$). This simplified model is beneficial in that it avoids the complexity of double-counting photons emitted by the sun, however leads to the nonintuitive conclusion that the ideal architecture of using a DC layer is to place it *below* the solar cell. While their analysis includes the possibility of placing the DC layer above the solar cell as well, including index-matching the layers,[6,8] their enhancement is optimized for the DC layer below the cell. This conclusion is undesirable for any solar cell since the increased absorption of high-energy photons implies that the photons with the potential to be down-converted will be absorbed *before* reaching the rear-DC layer. In this paper we analyze a more realistic system consisting of a pre-existing solar cell covered by a layer of down-converting nanoparticles. The use of particles and specifically nanoparticles is beneficial over the use of bulk DC materials proposed by others[5–8] since it is possible for nanoparticles to have a mid-energy band level that is required for a DC process.[9] Other advantages of using a nanoparticle DC layer are also discussed.

Our analysis follows the derivation method of Ruppel and Würfel[10] to calculate the open-circuit voltage and short-circuit current of the solar cell, thereby determining the efficiency. In Sec. II we fully analyze the DC system in the ideal (lossless) case, providing an ultimate efficiency improvement limit of 7% using the DC process. We then re-analyze the system while adding losses to the DC layer in Sec. III, providing the expected efficiency increase for a more realistic DC material. In Sec. IV we discuss the comparison with the thermodynamic approach devised by Markvart and

a)Author to whom correspondence can be addressed. Electronic mail: xiang@berkeley.edu.

Report Documentation Page

Form Approved
OMB No. 0704-0188

1. REPORT DATE	2. REPORT TYPE	3. DATES COVERED
06 JUN 2011		**00-00-2011 to 00-00-2011**

4. TITLE AND SUBTITLE	5a. CONTRACT NUMBER
Solar Energy Enhancement Using Down-converting Particles: A Rigorous Approach	5b. GRANT NUMBER
	5c. PROGRAM ELEMENT NUMBER
6. AUTHOR(S)	5d. PROJECT NUMBER
	5e. TASK NUMBER
	5f. WORK UNIT NUMBER
7. PERFORMING ORGANIZATION NAME(S) AND ADDRESS(ES) **University of California, Berkeley,NSF Nanoscale Science and Engineering Center,Berkeley,CA,94720**	8. PERFORMING ORGANIZATION REPORT NUMBER
9. SPONSORING/MONITORING AGENCY NAME(S) AND ADDRESS(ES)	10. SPONSOR/MONITOR'S ACRONYM(S)
	11. SPONSOR/MONITOR'S REPORT NUMBER(S)

12. DISTRIBUTION/AVAILABILITY STATEMENT
Approved for public release; distribution unlimited

13. SUPPLEMENTARY NOTES

14. ABSTRACT

The efficiency of a single band-gap solar cell is specified by the Shockley-Queisser limit, which defines the maximal output power as a function of the solar cell???s band-gap. One way to overcome this limit is by using a down-conversion process whereupon a high energy photon is split into two lower energy photons, thereby increasing the current of the cell. Here, we provide a full analysis of the possible efficiency increase when placing a down-converting material on top of a pre-existing solar cell. We show that a total 7% efficiency improvement is possible for a perfectly efficient downconverting material. Our analysis covers both lossless and lossy theoretical limits, as well as a thermodynamic evaluation. Finally, we describe the advantages of nanoparticles as a possible choice for a down-converting material.

15. SUBJECT TERMS

16. SECURITY CLASSIFICATION OF:			17. LIMITATION OF ABSTRACT	18. NUMBER OF PAGES	19a. NAME OF RESPONSIBLE PERSON
a. REPORT **unclassified**	b. ABSTRACT **unclassified**	c. THIS PAGE **unclassified**	**Same as Report (SAR)**	**9**	

Landsberg,[11,12] and show the self-consistency of these methods. In Sec. V we provide concluding remarks. Our analysis of the DC process demonstrates how the short-circuit current of the solar cell can be improved, while the open-circuit voltage remains largely unaffected. We furthermore provide a complete set of limits upon the measureable characteristics of the material, including both ideal and lossy systems.

II. DOWN-CONVERSION WITHOUT LOSSES

We first analyze the system without any losses in the DC layer as a maximized efficiency case. To analyze this system, we first define the fractions of light entering and exiting the system. Figure 1(a) displays the simplified band diagram of a DC material placed above a solar cell. In this system, a fraction of the photons are absorbed by the DC layer (f_{abs}), some are not absorbed (f_{NA}), with the photons that are absorbed being re-emitted as two lower energy photons (f_{dc}) via a midgap splitting level in the DC process. This splitting level does not need to be in the middle of the bandgap, but will be defined as such in order to simplify the derivation. While the fractions of photons not absorbed do not increase the number of electrons in the underlying solar cell, the DC ones increase the number of electron-hole pairs by one per down-converted photon. Neglecting losses and down-shifting, the fraction of photons absorbed by the DC material is equal to the fraction involved in DC: $f_{dc} = f_{abs} = (1 - f_{NA})$.

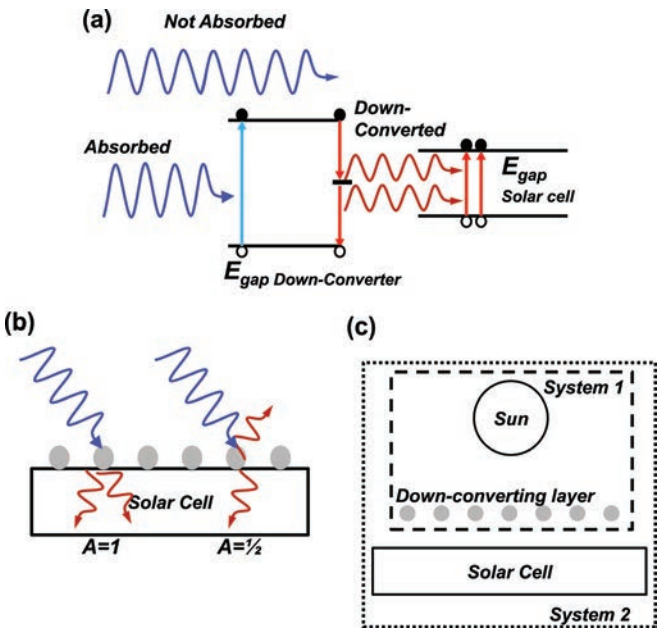

FIG. 1. (Color online) (a) Band diagram of the systems described, with a conversion layer having twice the band-gap of the underlying solar cell. Photons can either be not absorbed or absorbed and then down-converted. When down-conversion occurs, two electrons are created by the photon pair. (b) Schematic of a down-converting layer consisting of nanoparticles on top of a pre-existing solar cell. The down-converted photons can either be directionally scattered forward, resulting in a geometrical parameter, A, being unity, or half the down-converted photons can be scattered away from the solar cell, resulting in $A = 1/2$. (c) Schematic demonstrating the division of systems analyzed: System 1 includes the Sun and the down-converting media; System 2 includes the solar cell, with the light source emanating from System 1.

The DC nanoparticles act as photon scatterers. Therefore there is a probability of having some of the DC photons scatter away from the solar cell [see Fig. 1(b)]. To account for this, we will include a geometrical parameter, A, which can vary from $A = 1/2$ (isotropic emission) to $A = 1$ (directional emission), with A describing the portion of photons emitted *toward* the solar cell. This geometrical factor can be considered a component of the *optical étendue*,[13] since it describes the conservation of photons being emitted in a beam toward the solar cell. Clearly when $A = 1/2$ the additive efficiency capability of the DC process is negated since the number of photons eventually reaching the solar cell is conserved. However, this factor can be quite close to unity depending on the geometry of the system, as will be described in the discussion section. Naturally if the particles backscatter more than they transmit, then $A < 1/2$, but this case is clearly not of interest.

To analyze this system, we will use the open-circuit (o.c.) flow equilibrium method of Ref. 10: at o.c. no current is extracted ($I_{oc} = 0$) and therefore the photon flux absorbed must equal the photon flux emitted by the system. This equality of fluxes is used to establish the chemical potential (μ) of the system. Since the DC-solar cell system is more complex than a single-junction solar cell system, we divide the analysis into two parts, as delineated in Fig. 1(c). First we solve for the equilibrium condition for the first system, establishing the chemical potential and the photon flux of the DC process. Next, using the flux emitted from first system as a source for the second system, the chemical potential and efficiency of the solar cell are obtained.

Equating the photon flux coming from the sun using the Roosbroeck-Shockley Relation[14] (RSR), and the flux emitted by the DC material using its variation when including chemical potential,[15] we find:

$$f_{abs}\Omega_S \int_{2E_g}^{\infty} \frac{x^2 dx}{\exp(x/kT_s) - 1} = 4\pi n_{dc}^2 \times \frac{1}{2} \times f_{dc} \int_{E_g}^{\infty} \frac{x^2 dx}{\exp(x - \mu_{dc}/kT_{dc}) - 1} \quad (1)$$

Here, $f_{abs} = (1 - f_{NA})$ is the fraction of light absorbed, and is equal to f_{dc}, the fraction of light down-converted without losses; Ω_s is the solid angle subtended by the sun and is taken as 6.85×10^{-5} sr, with a refractive index of air ($n = 1$); $4\pi n_{dc}^2$ is the full-spherical 'cone' of light emitted from the DC layer (another component of the étendue); E_g and $2E_g$ are the band-gaps of the solar cell and DC layer, respectively; T_S and T_{dc} are the temperatures of the sun and DC layer, respectively; and k is the Boltzmann constant in eV units. The integral on the left is for a simple blackbody, following Planck's formulation, with only the light absorbed considered, hence the lower limit of integration at $2E_g$ (all light below $2E_g$ is transparent to the DC media). The right hand side models the DC layer as *two* photon sources emitting

with a pseudoband-gap of E_g, and a chemical potential of μ_{dc} using the RSR relation.[14,15] For two photon sources, the rate must be *half* that of a single junction solar cell to match the solar influx. This equation is nearly identical to that of a single junction solar cell, derived in Eq. (12) of Ref. 10 and can be used to establish the chemical potential of the DC layer.

System 2 in Fig. 1(c) has the output of System 1 as the light source for the solar cell, and consists of the fraction of nonabsorbed solar radiation, as well as the down-converted fraction. The o.c. condition[10] is once again found by equating the current flow to zero:

$$\Omega_S \int_{E_g}^{2E_g} \frac{x^2 dx}{\exp(x/kT_s)-1} + f_{NA}\Omega_S \int_{2E_g}^{\infty} \frac{x^2 dx}{\exp(x/kT_s)-1} + 2\pi n_{dc}^2 \times 2A \times f_{dc} \int_{E_g}^{\infty} \frac{x^2 dx}{\exp(x-\mu_{dc}/kT_{dc})-1} = 4\pi n_{sc}^2 \int_{E_g}^{\infty} \frac{x^2 dx}{\exp(x-\mu_{oc}/kT_o)-1} \tag{2}$$

Here, the first term is the light transparent to the DC layer, coming from the sun (a blackbody); the second includes the fraction not absorbed by the DC layer; the third term is the DC conversion providing $2A$ photons, at a hemispherical emission angle (since this equation only includes the flux *into* the solar cell); and the last term is the spherical emission from the solar cell (with temperature T_o). The geometric parameter, A, appears here as described above: for isotropic emission from the DC layer, it is equivalent to 1/2, whereas in directional emission it can be up to unity. Using Eqs. (1) and (2), we can also re-arrange the limits of integration of the first term to obtain:

$$\Omega_S \int_{E_g}^{\infty} \frac{x^2 dx}{\exp(x/kT_s)-1} + f_{dc}(2A-1)\Omega_S \int_{2E_g}^{\infty} \frac{x^2 dx}{\exp(x/kT_s)-1} = 4\pi n_{sc}^2 \int_{E_g}^{\infty} \frac{x^2 dx}{\exp(x-\mu_{oc}/kT_o)-1} \tag{3}$$

Here, we have assumed that $T_{dc}=T_o$, meaning that the DC layer and the solar cell are at thermal equilibrium. Equation (3) is identical to Eq. (12) in Ref. 10 for $f_{dc}=0$. This equation can be solved numerically for the o.c. voltage, $qV_{oc}=\mu_{oc}$, or a useful simplification can be done to derive a closed-form equation for V_{oc}. The maximal power point ($P_{\max}=I_{\max}\times V_{\max}$) can also be obtained by multiplying this equation by the voltage (and replacing μ_{oc} with V) and finding the maximum.[4] By neglecting the -1 term in the denominators of the integrands (i.e., for $x \gg kT_S$ and $x-\mu_{oc} \gg kT_o$), one can solve the definite integral for $qV_{oc}=\mu_{oc}$ and obtain a close approximation:

$$\mu_{oc} = E_g\left(1-\frac{T_o}{T_s}\right) + kT_o \ln\left[\left(\frac{\Omega_s}{4\pi}\right)\left(\frac{T_s}{T_o}\right)\right] + kT_o \ln\left(\frac{1}{n_{sc}^2}\right) + kT_o \ln(\alpha_1) + kT_o \ln(1+\beta_1) \tag{4}$$

With the parameters α_1 and β_1 defined as:

$$\alpha_1 \equiv 1 + \frac{2kT_s}{E_g} + \frac{2(kT_s)^2}{E_g^2}$$
$$\beta_1 \equiv f_{dc}(2A-1) \times 4\left(\frac{\alpha_2}{\alpha_1}\right)\exp\left(-E_g/kT_s\right) \tag{5}$$
$$\alpha_2 \equiv 1 + \frac{kT_s}{E_g} + \frac{(kT_s)^2}{2E_g}$$

Equation (4) is similar to the one derived for a single junction solar cell, [there, in Eq. (13) of Ref. 10 they obtain the first two terms of Eq. (4)], and it is also similar in form to Eq. (20) in Ref. 13. The added terms here are the index term, n_{SC}; a temperature and band-gap correction term, α_1; and an added term for DC, incorporating β_1. Both here and in the cited references, all terms containing kT_o/E_g are neglected. The β_1 factor can describe as a gain to the V_{oc} for any $A > 1/2$, and is equal to zero at hemispherical emission ($A=1/2$). It should be noted that equation (4) reverts back to Eq. (13) in Ref. 10, the solution for a single-junction solar cell, when $f_{dc}=0$, meaning for no DC. The individual contributions to each of the four rightmost terms in Eq. (4) are calculated in units of Volts at room temperature. The contribution of the α_1 term is mostly negligible, even at low band-gaps, since the integrands of Eq. (3) requires that $x > \mu_{oc}$, thereby pegging all low band-gap materials to $V_{oc}=0$ for $E_g < 0.2$ eV. Furthermore, the β_1 gain term is nearly zero for even full directional emission from the DC layer ($A=f_{dc}=1$). The index term is negative, contributing to a loss of V_{oc} due to the change in étendue of the emission from the solar cell into air. We further describe these expressions in terms of their thermodynamic significance in Sec. III.

Figure 2(a) displays the open circuit voltage as a function of gap energy for a numerical solution of Eq. (3) (solid black, curve 1), for a material with a constant refractive index of $n_{SC}=4$ and for the ideal case where $A=f_{dc}=1$, as well as V_{oc} for a regular solar cell (Eq. (3) with $f_{dc}=0$; solid blue, curve 2). To compare the numerical solution with the closed form approximation, we have also plotted Eq. (4) for the DC cell ($f_{dc}=1$; dotted black, curve 3) and for a regular cell ($f_{dc}=0$; dotted blue, curve 4). The V_{oc} for the DC cell is higher than the regular cell, regardless of the method used, with only a small difference between the two. The approximation of Eq. (4) is offset to the numerical solution by ~70 mV (black lines) at low E_g, and the regular cell solution is offset by ~100 mV (blue lines). The small gain contribution afforded by the β_1 term is only 5–15 mV for the numerical solution (solid lines), and 20–70 mV for the approximation (doted lines), with both sets of curves converging at high bandgap energies.

The primary increase in efficiency of the DC process lies in the increase in generation rate due to the doubling of number of photons with $E > 2E_g$. Calculating I_{sc} can be done using Eq. (2) with $\mu_{oc}=0$, and can be simplified by neglecting the re-emission from the solar cell and including only the incoming and DC photons,[16] since the re-emission from the solar cell at short-circuit is merely a blackbody with $T_o=300$ K. This increase per band-gap is displayed in

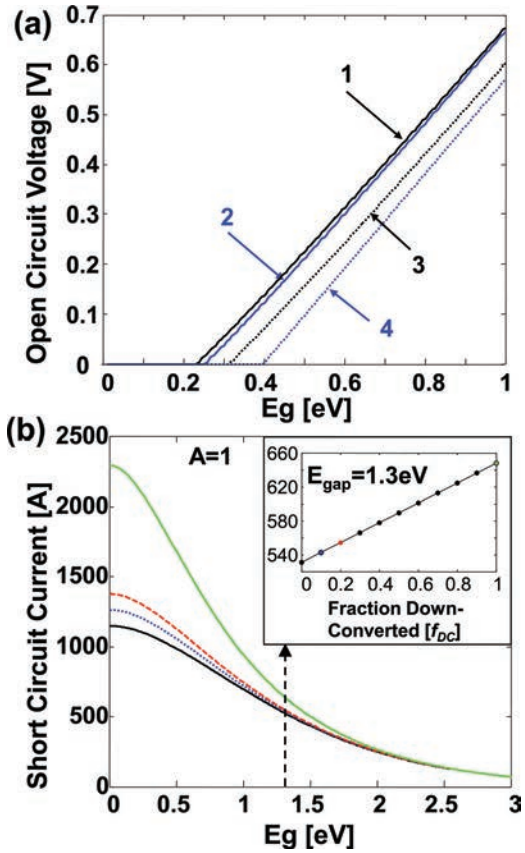

FIG. 2. (Color online) (a) Open circuit voltage versus the band-gap of the underlying solar cell, calculated numerically (solid lines) using Eq. (3); and using the approximation of Eq. (4) (dotted lines). Black lines are for a down-converting solar cell (curve 1, using the numerical solution, curve 3, using the approximation), and blue lines are for a regular solar cell as calculated with $f_{dc}=0$ (curves 2 and 4, numerical and approximation, respectively). (b) Short circuit current versus bandgap for the ideal case where $A=1$, for varying values of f_{dc}: solid black −0%, which is equivalent to a regular solar cell without down-conversion; dotted blue −10%; dashed red −20%; solid green −100%. Inset: For a set band-gap value of 1.3 eV (dashed arrow), the increase in current as a function of f_{dc} is shown.

Fig. 2(b), indicating that I_{sc} can be doubled at zero band-gap. This would nevertheless provide zero efficiency, since the efficiency of the solar cell is a product of I_{sc} with V_{oc}, with V_{oc} proportionate to the band-gap as demonstrated above. For a Gallium-Arsenide solar cell, one can expect over a 120 A increase in I_{sc} for 100% DC efficiency [$f_{dc}=1$; Fig. 2(b), inset].

To calculate the overall efficiency of the system, one needs both V_{oc} and the short-circuit current, I_{sc}, in addition to the Fill-Factor:

$$\eta_{eff} = FF \times I_{sc} \times V_{oc} \tag{6}$$

With the Fill-Factor given by Green's[17] approximation, which is considerably accurate:[18]

$$FF = \frac{v_{oc} - \ln[v_{oc} + 1 - \ln(v_{oc})]}{v_{oc} - \ln[v_{oc} + 1 - \ln(v_{oc})] + 1} \times \frac{v_{oc} - \ln\{v_{oc} - \ln[v_{oc} + 1 - \ln(v_{oc}) + 1\}}{v_{oc}[1 - \exp(-v_{oc})]} \tag{7}$$

where $v_{oc} = V_{oc}/kT_o$, using V_{oc} calculated numerically from Eq. (3).

Figure 3 shows the efficiency versus solar cell band-gap for three different values of A, and different values of DC efficiency[19] (f_{dc}). For the isotropic emission case, with $A = 1/2$ [Fig. 3(a)], there is no difference in varying f_{dc}, and all efficiency curves overlap. For rising values of A, greater DC efficiency results in improved overall efficiency. Figures 3(b) and 3(c) show the increase in efficiency for rising values of f_{dc}, with a subsequent leftward shifting of the ideal underlying solar cell band-gap. The lowest curve in each (solid black) is for zero DC contribution ($f_{dc}=0$), corresponding to a single junction solar cell, and is identical to the curve in Fig. 3(a). However, increases of f_{dc} by 10% (blue and red, at 10% and 20%, respectively) can increase the overall efficiency of the system, with an ultimate limit corresponding to the topmost

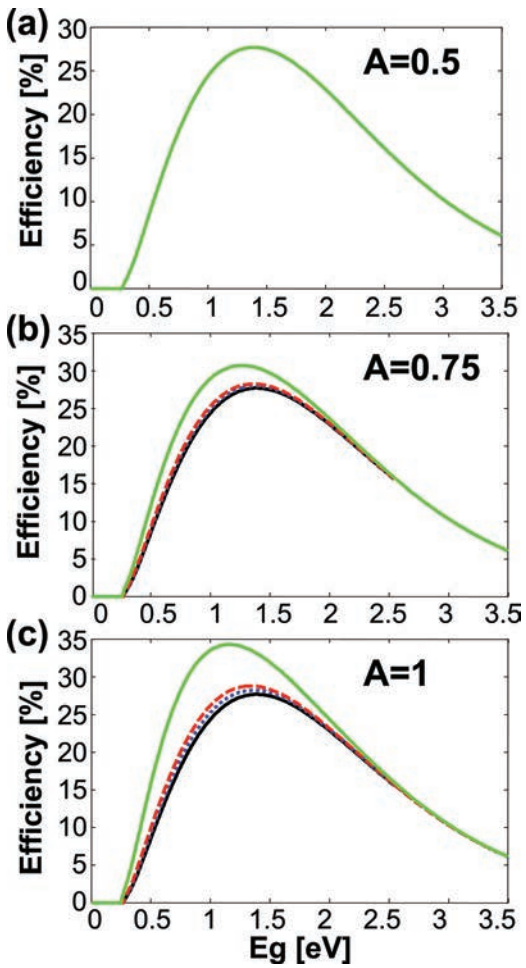

FIG. 3. (Color online) Efficiency curves for three values of the geometrical parameter, A. (a) With $A=0.5$, half the down-converted photons are emitted away from the solar cell, thus resulting in no net gain, regardless of the down-conversion fraction. Here, all curves overlap, with a maximal efficiency of 27.7% using a constant index of refraction: $n=4$. (b), (c) Efficiencies with varying fractions of down-conversion efficiency, for geometrical factors of $A=0.75$ (b), and $A=1$ (c). In each plot, the lowest curve (solid black) is for $f_{dc}=0$, identical to panel (a), the result for a single junction solar cell. The curves above it are for rising fractions of down-conversion: $f_{dc}=10\%$ (dotted blue), $f_{dc}=20\%$ (dashed red) and $f_{dc}=100\%$ (solid green). Maximum efficiency with $A=1$ and $f_{dc}=100\%$ is 34.3%.

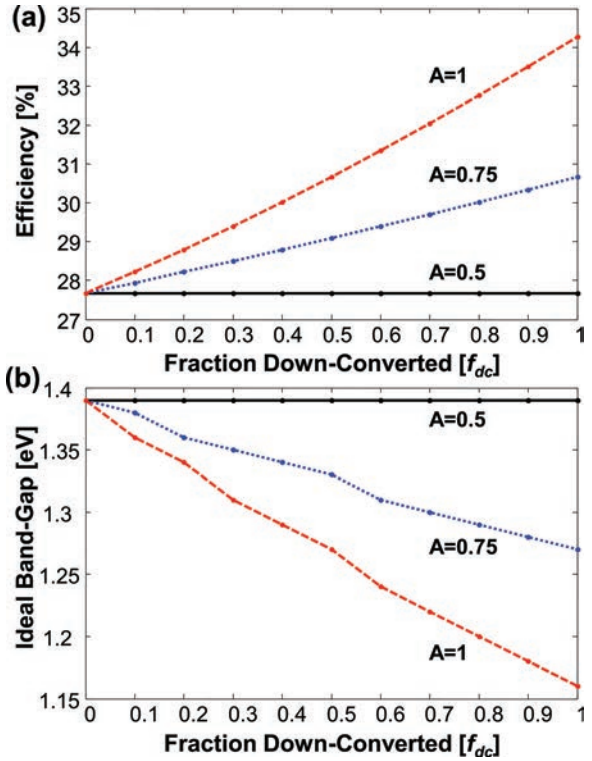

FIG. 4. (Color online) (a) Efficiency as a function of the down-conversion fraction, for three values of the geometrical factor, A. The efficiency rises monotonically, as calculated by maximizing the efficiency formula (6). (b) Ideal band-gap of the underlying solar cell, as a function of the down-conversion fraction. For higher down-conversion ratios, the ideal band-gap is lowered to more effectively utilize the solar spectra.

green curve in each panel when $f_{dc}=1$. For maximal directionality ($A=1$), and maximal efficiency of DC ($f_{dc}=1$), the upper limit is ~34.3%, providing an absolute increase of 7% from the single junction limit of 27.7% (using $n_{SC}=4$).

To further elucidate the relation between DC efficiency, underlying band-gap and overall efficiency, we plot in Fig. 4(a) the rise in efficiency as a function of the fraction of photons down-converted (with $f_{dc}=1$ corresponding to all absorbed photons being down-converted). For hemispherical emission from the DC layer ($A=1/2$, solid black), no change in efficiency is calculated since half of the DC photons are scattered away from the solar cell. However, for full directional emission ($A=1$, dashed red) the 7% rise in efficiency is apparent. In Fig. 4(b) we plot the ideal band-gap as a function of the DC fraction, with the ideal band-gap being the maximum of the efficiency curves. Larger fractions of DC efficiency correspond to a *lower* preferred band-gap of the underlying solar cell. Note however that this number does not drop below 1.1 eV, which conserves the preferred band-gap of the solar cell within the Si/GaAs region.

III. DOWN-CONVERSION WITH LOSSES

Accounting for losses is achieved by multiplying the photon flux equilibrium of System 1 in Fig. 1(c) by the external quantum efficiency[20] of the down-conversion process:

$$f_{adc}\Omega_S\int_{2E_g}^{\infty}\frac{x^2dx}{\exp(x/kT_S)-1}=4\pi n_{sc}^2\times\frac{1}{2k}\times\int_{E_g}^{\infty}\frac{x^2dx}{\exp(x-\mu_{dc}/kT_{dc})-1} \quad (8)$$

where the external quantum efficiency, K, is defined by:

$$K=\frac{f_{dc}}{f_{abs}}=\frac{f_{dc}}{f_{dc}+f_L} \quad (9)$$

with f_L being the loss fraction. Since $f_{dc}+f_L=f_{abs}\leq 1$ the external quantum efficiency of this DC process need not reach unity for all values of DC, f_{dc} and loss, f_L.

Following the identical procedure of the lossless case, placing Eq. (8) in Eq. (2), we can solve for $qV_{oc}=\mu_{oc}$:

$$\mu_{oc}=E_g\left(1-\frac{T_o}{T_s}\right)+kT_o\ln\left[\left(\frac{\Omega_s}{4\pi}\right)\left(\frac{T_s}{T_o}\right)\right]+kT_o\ln\left(\frac{1}{n_{sc}^2}\right)+kT_o\ln(\alpha_1)+kT_o\ln(1+\beta_2) \quad (10)$$

With α_1 defined as before in Eq. (5), and β_2 defined by:

$$\beta_2\equiv f_{dc}(2KA-1)\times 4\left(\frac{\alpha_2}{\alpha_1}\right)\exp(-E_g/kT_s) \quad (11)$$

As can be seen, the only difference between the lossy case and the lossless case is the additional multiplication of the geometrical parameter, A by K, the external quantum efficiency of the overall DC process. However, this system is now a function of *three* free parameters: A, f_{dc} and f_L; with K defined by both f_{dc} and f_L. The current is likewise nearly equivalent to Eq. (3), with the replacement of the factor $(2A-1)$ with $(2KA-1)$ to account for the losses. The losses included in the factor K do not include the backscattering losses already included in the geometrical factor, A, with the $2KA$-1 ensemble appearing in the β_2 term in Eq. (11). Losses can include impedance mismatches between the index of refraction of the DC layer and the solar cell,[6,7] but are generally the product of nonradiative recombination between the internal bands in the DC material,[20] or impurities in the DC material.[21]

The efficiency is calculated the same way as in the lossless case using Eq. (6), as a function of f_{dc}, f_L and A. Fig. 5 plots the efficiency curves for four different value pairs of f_{dc} and f_L [$f_{dc}=0.1$, $f_L=0.1$ in (a); $f_{dc}=0.2$, $f_L=0.1$ in (b); $f_{dc}=0.5$, $f_L=0.1$ in (c); and $f_{dc}=1$, $f_L=0$ in (d)], and plotting for three values of the geometrical parameter, A ($A=0.5$ in solid black, $A=0.75$ in dotted blue and $A=1$ in dashed red). The same increase in efficiency can be seen here, with the ideal lossless case [$f_{dc}=1$ and $f_L=0$, in (d)] appearing in Fig. 5(d) being identical to the ideal lossless case depicted in the topmost green curves in Fig. 3. The efficiency increase including losses is far less substantial than the lossless case. For example a lossy material with 20% DC efficiency, but 10% loss, as in Fig. 5(b), will only have a maximal ~0.5% increase for fully directional emission.

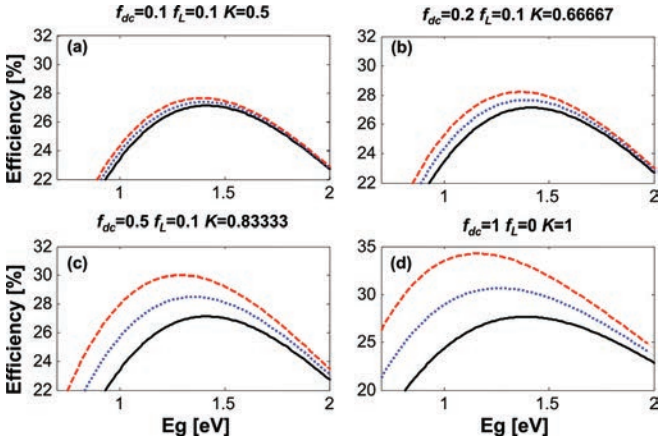

FIG. 5. (Color online) Efficiencies including losses, for four values of down-conversion and loss fractions, f_{dc} and f_L, respectively. The quantum efficiency is: $K=f_{dc}/(f_{dc}+f_L)$. In each panel, black (solid) line is for the geometrical factor $A=0$, blue (dotted) for $A=0.75$ and red (dashed) for $A=1$. For each, at $A=1$, maximal efficiency is: (a) 27.7%; (b) 28.2%; (c) 30%. Panel (d) is identical to Fig. 3(c), with an increase to 34.32% from 27.67%.

To better understand these results, we plotted in Fig. 6 the efficiency for $A=0.75$ and $A=1$, as a function of the two parameters: f_{dc} and f_L. For no loss, the nominal efficiency of the solar cell would here be 27.7%, with no DC occurring. Increasing the loss without simultaneously increasing the DC efficiency corresponds to a *drop* in efficiency below 27.7%. The maximal efficiency is 34.3% (increased from 27.7%), similar to the lossless result, and appears as the top-leftmost point in both panels, corresponding to full DC, and no loss. Drawn on each panel of Fig. 6 is the threshold for improving the efficiency: anything below this threshold has a *lower* efficiency than a single junction solar cell, corresponding to a loss in absorption by the DC layer, whereas anything above this threshold has a higher efficiency. As can be seen, the threshold slope decreases with higher ratios of directionality ($A\rightarrow 1$). This result can intuitively be inferred from the DC gain factor of $(2KA-1)$: in order to obtain any gain in current, the external quantum efficiency of DC conversion must surpass the losses in étendue due to nondirectional emission.

The internal quantum efficiency measurable using a spectrometer is different from the definition of external quantum efficiency, K described above in Eq. (9). When measured in isolation, the quantum efficiency (QE) of the DC material will vary from zero to unity, such that $QE \leq K$. The relation between QE and K is: $QE \equiv \{K|f_{NA}=0\}$, which coincides with the hypotenuse of the triangular graphs in Fig. 6, as depicted by the color-coded arrows in Figs. 6(a) and 6(b). We plot the efficiency versus QE in Fig. 7 for both $A=0.75$ (blue) and $A=1$ (red), including the 27.7% efficiency limit (dashed black line). These lines follow the trajectory of the arrows in Fig. 6.

In Fig. 7, anything below the dashed line corresponds to a reduction in efficiency caused by the surplus of loss in the DC material. For a DC material to provide any advantageous capabilities, their measured QE must be approximately greater than 50%. For $A<1$, the QE must be greater than 60–70% for any real benefit to be detected. Including losses due to lack of absorption by the DC layer ($f_{NA} \neq 0$) will further reduce the efficiency increase as shown in Fig. 6.

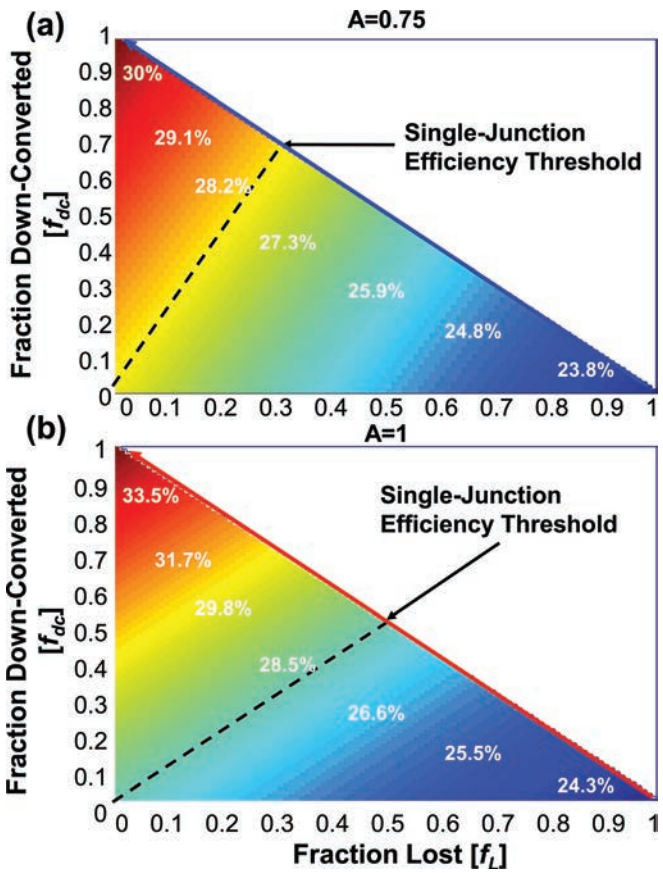

FIG. 6. (Color online) Efficiency for $A=0.75$ (a), and $A=1$ (b), for varying loss and down-conversion fractions. Efficiencies are also displayed on the graph itself. Dashed lines represent the efficiency curve for a single junction solar cell; all points to the right of this curve represent reduced efficiencies and those to the left represent the improved efficiencies.

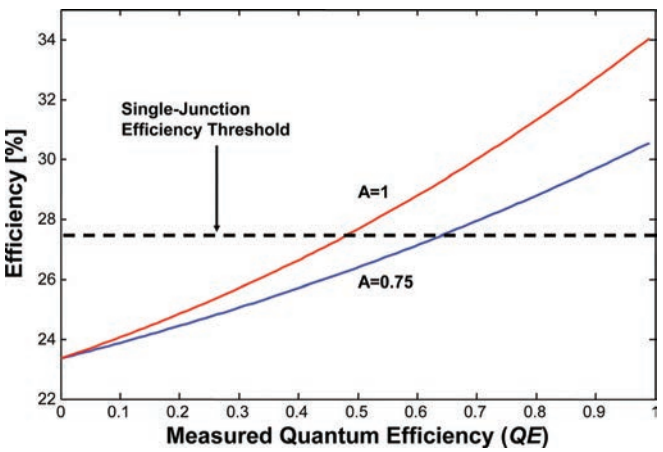

FIG. 7. (Color online) Efficiency per quantum efficiency, disregarding not absorbed light ($f_{NA}=0$), for two different values of the geometrical factor, A. The 27.7% efficiency threshold corresponding to a single junction solar cell is also displayed, signifying the partition between regions of gain and loss.

IV. DISCUSSION

Analysis of the efficiency of solar cells can be restated by using basic thermodynamic arguments (see Refs. 11, 20, 22, and 25 for a review). In this approach, the Fill-Factor and I_{sc} remain the same, but a more basic thermodynamic derivation is used to describe V_{oc} using the Gibbs free energy (G) and appropriate loss of entropy (S). By equating the maximal voltage obtainable, V_{oc}, with the excess free energy in the solar cell conversion system, δG,[11] one can make simple arguments to derive Eqs. (4) and (10). The maximal voltage obtainable can be no larger than the band-gap voltage times the Carnot efficiency[23,24] which immediately provides the first term in Eqs. (4) and (10): $U = E_g(1 - T_o/T_s)$. Further losses/gains to V_{oc} are given by the change in entropy multiplied by the temperature of the solar cell, resulting in terms appearing as $kT_o \times ln(\cdot)$, since $\mu_{oc} = \delta G = U - TS$. The entropy, S, can be considered as the internal information inherent to the system, and also measures the reversibility of a process.

The first loss term appearing in Eqs. (4) and (10) are due to the change in étendue of the beam[13] subtending from the sun and then converted into a spherical source emanating from the solar cell, $(\Omega_s/4\pi)$. This term can include the effects of concentration, with the loss of nonconcentrated solar light resulting in a constant -0.31 V loss. Moderate concentration can improve this loss dramatically.[26] The second term is a temperature difference from conversion of solar temperatures to ambient ones, (T_S/T_o), and raises the voltage by 0.077 V. These two terms combine to a constant loss of -0.23 V for nonconcentrated light, losses that will occur regardless of the choice of solar cell material.

The index term loss, $(1/n_{SC}^2)$ varies with material choice to further reduce V_{oc} by approximately -0.07 V (averaged, using the measured index of Si.[27] This term can be increased due to internal reflections, as shown by Yablonovitch and Cody,[28] resulting in an increase of losses to approximately -0.1V $(1/n_{SC}^2 \rightarrow 1/4n_{SC}^2)$. This term is due to loss of étendue from the reflection of a portion of the incoming (and outgoing) light at the interface.

The DC process was shown in Fig. 2 to have minimal contribution to V_{oc}. Since β_1 and β_2 are very small, the additional voltage component obtained is near zero, and can in fact be *negative* for lossy DC processes [i.e., if the term $(2KA-1) < 0$]. The thermodynamic meaning of this term can be found by rewriting this expression in terms of the photon fluxes, $N(E)$, as a function of the energy using the RSR:

$$N(E_g) = \text{const} \int_{E_g}^{\infty} \frac{x^2 dx}{\exp(x/kT_s) - 1} \approx \text{const} \times kT_s E_g^2 \alpha_1 \exp(-E_g/kT_s) \tag{12}$$

The approximation in Eq. (12) is the same as that described above, neglecting the -1 in the denominator. If the lower limit, E_g, is replaced by $2E_g$, then the α_1 term in Eq. (12) is replaced by α_2, as described in Eq. (5). Examining the definition of β in Eqs. (5) and (11), we can see that β can be rewritten in terms of N, for $N(E_g)$ and $N(2E_g)$, since:

$$\frac{N(2E_g)}{N(E_g)} \approx 4\left(\frac{\alpha_2}{\alpha_1}\right) \exp(-E_g/kT_s) \tag{13}$$

Using such a description, we obtain for the entropy of the ideal DC process that:

$$S_{dc} \equiv k \times \ln(1 + \beta_2) = k \times \ln\left[\frac{N(E_g \rightarrow 2E_g) + 2KA \times N(2E_g)}{N(E_g)}\right] \tag{14}$$

Here, the term $N(E_g \rightarrow 2E_g)$ is the number of photons in the range $E_g \rightarrow 2E_g$ in the solar spectrum. This result can only be obtained for $f_{dc} = 1$, in the ideal case.

The physical meaning of Eq. (14) can be understood as simply the ratio of the number of photons impinging upon the solar cell, to the total number of photons initially emitted toward the solar cell (and absorbable by it). The added entropy is therefore due to the addition of a "particle" to the system, thereby increasing the disorder. The factor $2KA$ is therefore the source of entropic gain: if $2KA > 1/2$, then there is an additional photon created, resulting in an increase of entropy (or disorder. This refers to the external system, System 1 in Fig. 1(c), with the solar cell's entropy being reduced, thereby increasing δG). However, if $2KA = 1/2$, the numerator and denominator are equal, resulting in no gain or loss of entropy.

Finally, an additional term can be added to the V_{oc} formula to include the quantum efficiency of the solar cell that includes nonradiative losses.[25] This additional term, $kT_o \ln(1/QE_{SC})$, can be relatively large for a material such as Silicon. The contribution of the additional term including α_1 in Eqs. (4) and (10) has no entropy equivalent, and is generally ignored in thermodynamic comparisons.[13] Neglecting this term is relatively harmless, as it introduces a "gain" of approximately 0.024 V for a 1 eV band-gap solar cell. It appears in Eq. (4) due to the definite integral solution obtained when neglecting the -1 in the denominator of the Planck/Bose-Einstein/RSR distribution.

The results of both approaches are therefore self-consistent, excluding the α_1 contribution (negligible), demonstrating that the DC process does not add any significant entropic loss. The reversibility of the DC process is nevertheless not assured for even the ideal (lossless) material, since the time-reversal process of recombining two DC photons into a single high energy one is functionally not one-to-one. This is because two different higher energy photons $(hv_1 \neq hv_2)$ will produce the same DC photon pair, despite the energetic (and entropic) differences between them; whereas, in the reverse process two lower energy photons will not reproduce those same photons. This entropic loss does not appear here since we have associated no losses to the thermalization process itself, which generates heat and thus entropy.

Down-shifting is another closely related process that has been suggested for improving single junction solar cells. Down-*converting* is different from down-*shifting*, whereby higher energy photons are absorbed and then reemitted at lower energies via a fluorescent process. Down shifting is another way for increasing solar cell efficiency since these

higher energy photons would otherwise be absorbed at the solar cell's surface, beyond a diffusion length from the internal *pn*-junction (and within a diffusion length of the surface), and would therefore not contribute to the overall current of the solar cell. This type of system was first proposed by Yablonovitch[29] and further analyzed by Markvart,[30] however it is designed to improve the efficiency of existing solar cell systems by approaching the Shockley-Quiesser limit, and not intended to surpass that limit. Adding down-shifting to this analysis can be obtained by adding another parameter to our equations, the down shifting efficiency f_{ds}. However, it would not fundamentally change the concepts provided here.

An additional advantage of using semiconducting nanoparticles lies in the geometrical term, A. For a flat solar cell, placing any DC coating on top of the solar cell would result in a loss of half the photons,[5,7] such that $A \approx 1/2$. However, if instead nanoparticles are embedded within the top layer of the solar cell then $A > 1/2$, since scattering is then inconsequential. In this case, the refractive index of the nanoparticles will need to be considered, since there would be preferred impedance matching between the DC material and the solar cell.[7,8] An additional geometry would be in liquid (dye-based) solar cells, whereupon the nanoparticles can be embedded within the solar cell itself, as in Fig. 8(a). In this geometry, only those DC nanoparticles at the surface will lose half of their photons to the outside—without considering the internal reflection at the interface. Furthermore, a DC nanoparticle system would be ideal in a micro- or nano-pillar system,[31,32] as in Fig. 8(b), where the scattering of the DC light is advantageous. In such a system, the nanoparticles would act as both a scatterer and a spectral-splitter. This advantage in geometry would be true for any three-dimensional configuration of the DC layer, as opposed to the two-dimensional solar cell.

The postulated use of nanoparticles as a DC layer has yet to be fully studied. The requirements for a DC layer are in the high concentration of mid-band-gap "splitting" states that are *both* radiative. It has been shown theoretically that there is a threshold for trap-concentrations in semiconductors beyond which the mid-level trap states coalesce into a band, and become doubly radiative.[9] This process was deemed desirable for use in an intermediate-level solar cell.[33] A single radiative process is similar to the Stokes shift in a fluorescent process, whereas a doubly nonradiative process is typically what occurs at a nonpassivated surface. There are currently no known efficient doubly radiative materials, with the DC process having been demonstrated only in materials doped with lanthanides,[34,35] at extremely low efficiency, and requiring high input energy. However, for semiconducting nanoparticles, the high surface-to-volume ratio may possibly be a method of creating a high concentration of such mid-level trap states that function in this doubly radiative process in an efficient manner. In such a material system, the increase in surface traps could be thus advantageous for the DC process.

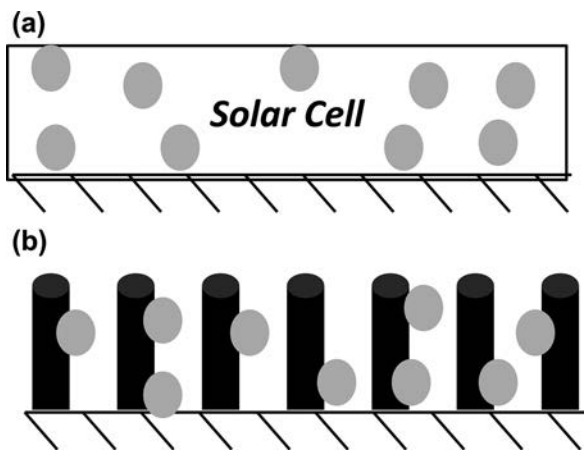

FIG. 8. Schematics of configurations offering improved directionality of the down-converted light emitted by the nanoparticles. (a) Nanoparticles embedded within a liquid solar cell (dye-sensitized, etc.); (b) nanoparticles embedded within a micro/nano-pillar solar cell.

V. CONCLUSIONS

We show here the enhancement capabilities of down-conversion, taken with and without losses, in the absence of any concentration. The total absolute enhancement of efficiency is up to 7% in an ideal system. The limit of this increase to 7% is due to the inherent limitation in the down-conversion process whereby choosing the underlying solar cell's band-gap to best match the solar spectrum consequently limits the number of high energy photons at twice that band-gap. We show that the DC process increases the short-circuit current, while retaining the open-circuit voltage, as the DC process does not introduce any significant entropy losses. We posit the use of nanoparticles as such a material system, due to its possibility of containing doubly radiative emission processes, and its advantages in solving the inherent scattering property of a down-converting layer. The results displayed in Figs. 6 and 7 provide the parameter space of the measureable quantities for a realistic DC material. The improvement in possible efficiency using a candidate DC material can be directly measured from the spectrum of the material, finding the DC and loss ratios as a function of the material's *QE*. As there has yet to be found a material system where down-conversion can occur efficiently, this paper delineates the measurable properties of the material system that will enable any form of efficiency enhancement.

ACKNOWLEDGMENTS

The work was supported by the U.S. Department of Energy, Basic Energy Sciences Energy Frontier Research Center (DoE-LMI-EFRC) under award DOE DE-AC02-05CH11231 and by the National Science Foundation Nano-Scale Science and Engineering Center (NSF-NSEC) under award CMMI- 0751621. ZRA acknowledges the National Defense Science and Engineering Graduate (NDSEG) Fellowship, 32 CFR 168a. Thanks to Majid Gharghi, Christopher Gladden, Owen Miller, and Eli Yablonovitch for their helpful discussion.

[1]W. Shockley and J. K. Queisser, J. Appl. Phys. **32**, 510 (1961).
[2]M. Wolf, Energy Convers **11**, 63 (1971).

[3]M. Wolf, Proceedings of the Institute of Radio Engineers **48**, 1246 (1960).
[4]M. A. Green, *Third Generation Photovoltaics* (Springer-Verlag, Berlin, 2003).
[5]T. Trupke, M. A. Green, and P. Würfel, J. Appl. Phys. **92**, 1668 (2002).
[6]V. Badescu, A. De Vos, A. M. Badescu, and A. Szymanska, J. Phys. D: Appl. Phys. **40**, 341 (2007).
[7]V. Badescu and A. De Vos, J. Appl. Phys. **102**, 073102 (2007).
[8]A. De Vos, A. Szymanska, and V. Badescu, Energy Convers. Manage. **50**, 328 (2009).
[9]A. Luque, A. Martí, E. Antolín, and C. Tablero, Physica B **382**, 320 (2006).
[10]W. Ruppel and P. Würfel, IEEE Trans. Electron Devices **27**, 877 (1980).
[11]T. Markvart and P. T. Landsberg, *Proceedings of the Third World Conference on Photovoltaic Solar Energy Conversion*, Osaka, Japan, 2003, p. 289.
[12]E. Yablonovitch, private communication (2010).
[13]T. Markvart, J. Opt. A: Pure Appl. Opt. **10**, 015008 (2008).
[14]W. van Roosbroeck and W. Shockley, Phys. Rev. **94**, 1558 (1954).
[15]G. Lasher and F. Stern, Phys. Rev. **133**, A553 (1964).
[16]Calculating the short circuit current can be done using Eq. (3), with the right hand side being 5 orders of magnitude smaller (blackbody at 300K). To get units of current [A], multiply this equation by $^2\Omega_{SQ}q/c^2h^2$, when using units of eV, equaling a constant of ~3452.65 A/m_2, considering an area of 1 m^2.
[17]M. A. Green, Sol. Cells **7**, 337 (1982).
[18]The Fill-Factor for a cell with multiple DC layers (or carrier multiplication) approaches unity, similar to the Fill-Factor for a cell with high concentration. Calculating the efficiency for multiple layers requires calculating Pmax for Eq. (3), after multiplying by V, as described in Ref. 4. The difference between this solution and the one using the Fill-Factor of Ref. 17 is less than 0.1%, with the results of maximal efficiency increase of 6.6% using the DC layer as opposed to 6.7%.
[19]To calculate the efficiency, the integral $[x^2dx/(\exp(x/kT_S) -1)]$ was evaluated, and then multiplied by a constant of $15/(\pi kT_S)^4$, which, when used in conjunction with the FF and Voc listed, provide the correct units. This assumes a unit area of unity. Integrals were calculated using the quadgk function in Matlab, which is better for solving integrals with known poles.
[20]R. T. Ross, J. Chem Phys. **46**, 4590 (1967).
[21]Q. Y. Zhang and X. Y. Huang, Prog. Mater. Sci. **55**, 353 (2010).
[22]T. Markvart, Appl. Phys. Lett. **91**, 064102 (2007).
[23]P. T. Landsberg and T. Markvart, Solid State Electron. **42**, 657 (1998).
[24]P. T. Landsberg and V. Badescu, J. Phys. D: Appl. Phys. **33**, 3004 (2000).
[25]T. Markvart, Phys. Status Solidi A **205**, 2752 (2008).
[26]M. Peters, J. C. Goldschmidt, and B. Bläsi, Sol. Energy Mater. Sol. Cells **94**, 1393 (2010).
[27]Silicon refractive index data extrapolated from: http://pvcdrom.pveducation.org/index.html, Appendix 3.
[28]E. Yablonovitch and G. D. Cody, IEEE Trans. Educ. **29**, 300 (1982).
[29]E. Yablonovitch, J. Opt. Soc. Am. **70**, 1362 (1980).
[30]T. Markvart, J. Appl. Phys. **99**, 026101 (2006).
[31]B. M. Kayes, H. A. Atwater, and N. S. Lewis, J. Appl. Phys. **97**, 114302 (2005).
[32]E. Garnett and P. Yang, Nano Lett. **10**, 1082 (2010).
[33]A. Luque and A. Martí, Phys. Rev. Lett. **78**, 5014 (1997).
[34]R. T. Wegh, H. Donker, K. D. Oskam, and A. Meijerink, Science **283**, 663 (1999).
[35]B. M. van der Ende, L. Aarts, and A. Meijernik, Phys. Chem. Chem. Phys. **11**, 11081 (2009).